

# A three-dimensional drift pushover method for unsymmetrical plan buildings

Mehdi Karimi<sup>1</sup> · Farhad Behnamfar<sup>1</sup> 

Received: 12 August 2017 / Accepted: 31 January 2018 / Published online: 5 February 2018  
© Springer Science+Business Media B.V., part of Springer Nature 2018

**Abstract** The drift pushover analysis method for tall and regular buildings is extended in this paper to the third dimension. The focus of study is on the structures with important torsional response. For this purpose, 10, 15, 20 and 30-story steel moment frame buildings having unsymmetrical plans with 5–30% eccentricity ratios are studied. For evaluation of accuracy, nonlinear dynamic response of the buildings is determined under a consistent suit of earthquake ground motions. The maxima of the story drifts and shears and cumulative plastic hinge rotations of stories are calculated under the ground motions and their averages along with those of the modal pushover procedure are compared with the results of the presented method. The comparative analysis establishes the good accuracy of the three dimensional drift pushover method.

**Keywords** Drift pushover · Three-dimensional · Unsymmetric · Tall · Nonlinear dynamic

## 1 Introduction

The nonlinear static, or pushover, analysis method has been established as an approximate and more practical substitute for the exact but cumbersome nonlinear dynamic analysis procedure. The conventional pushover method is mainly useable only for the structures for which just the fundamental mode governs the total dynamic response. In recent years, many attempts have been performed to overcome this limitation and extend the pushover method to be used for tall and/or irregular buildings. The approaches taken can be divided in two categories.

In the first category, it has been tried to modify the pattern of the lateral load distribution as the structure assumes more and more extensive nonlinear response by using its

---

✉ Farhad Behnamfar  
farhad@cc.iut.ac.ir

<sup>1</sup> Department of Civil Engineering, Isfahan University of Technology, Esfahan 8415683111, Iran

momentary mode shapes. This approach is called the adaptive pushover. The methods proposed by Bracci et al. (1997), Gupta (1999), Gupta and Kunnath (1999), Requena and D'Ayala (2000), Antoniou and Pinho (2004) and others are among the different adaptive methods.

In the second category, while the simplicity is retained by use of the initial elastic dynamic properties of a structure, effects of higher modes are included one way or another. This approach is called the mode-based pushover analysis. The mode-based approach has been implemented in several variations. Chopra and Goel (2000) presented a force-based alternative called the modal pushover analysis (MPA) method in which the lateral response was calculated by combining those of several pushover analyses each one for a certain mode of vibration. Extension of the MPA method to unsymmetric-plan buildings was made by Chopra and Goel (2004). Afterwards, Reyes and Chopra (2011a, b) extended the procedure to 3D eccentric buildings subjected to bi-directional ground motions within the framework of the practical modal pushover analysis (PMPA). The method was called practical because a major simplification was made to its predecessor by determining the seismic demands directly from a design acceleration spectrum, not by performing non-linear dynamic analysis.

A significant fact that differs the 3D pushover from the previous 2D ones is that in unsymmetric buildings a single target displacement is no longer sufficient to describe the lateral behavior. The reason is clearly because the torsional resonance results in simultaneous amplification and reduction of the displacement demand at the two opposite sides of a story. In this line of thinking, Tso and Moghadam (1997) and Moghadam and Tso (2000a, b) developed a procedure for one-way unsymmetric buildings subjected to single-component excitations. In their method, the target displacement of each lateral system is determined using an elastic response spectrum analysis. Then the associated load patterns are calculated and a 2D pushover analysis is performed for each system.

In a similar framework, an important development for inclusion of torsional effects into pushover analysis was made by Fajfar et al. (2005a, b) with introducing an extended version of their original 2D pushover procedure called the N2 method. In the extended version, a linear elastic analysis was performed to calculate the torsional amplification of lateral displacements at the corners of plan, assuming that the elastic design spectrum is conservative with respect to the inelastic one.

Albanesi et al. (2002), Parducci et al. (2006), and Tjhin et al. (2005) developed energy-based variations of the mode-based pushover procedure. In their methods, it was attempted to retain the expected maximum kinetic energy of vibration in the nonlinear static analysis.

In the displacement-based variation, the modal displacements or drifts of stories have been taken as the basis of pushover analysis. The works of Antoniou and Pinho (2004), Poursha et al. (2009), Sahraei and Behnamfar (2014) and Behnamfar et al. (2016) are within the mentioned approach. For instance, in the drift pushover analysis (DPA) proposed in reference (Behnamfar et al. 2016), first the maximum modal drifts were calculated using conventional procedures. Then, a combined story drift was determined by simple summation of modal responses and use of a modal correction factor, for each story in each mode. The above procedure was used instead of SRSS or CQC to retain the sign of modal responses when combining their values. Several approaches were tested for calculation of the modal correction factor and the one with an accuracy superior to other well-known procedures, like MPA, was identified. An equivalent lateral load pattern consistent with the distribution of story drifts was also proposed. For a class of 2D regular buildings, it was shown that the proposed pushover procedure could suitably follow the averaged maximum nonlinear responses of studied structures under a suit of consistent ground motions.

In line with the method proposed by Behnamfar et al. (2016), in this paper the DPA procedure is applied to torsional 3D buildings with mass eccentricity in plan. Several eccentricity ratios and several approaches for combination of modal drifts are examined. Moreover, effect of distribution pattern of the equivalent lateral forces is explored using two different alternatives. Accuracy of the nonlinear story responses is studied by comparison with the exact nonlinear time history analysis (NTA) responses calculated as the average of maximum nonlinear dynamic responses of the buildings under a consistent suit of ground motions.

## 2 Formulation of the method

The DPA procedure is implemented in four different steps (Behnamfar et al. 2016):

1. Calculate the maximum story drifts in each mode using the mass and (elastic) stiffness properties of the structure.
2. Add the modal drifts and calculate a unique maximum story drift by including contribution of at least the important modes and retaining the signs of modal responses. A modal combination factor is introduced for this purpose. The important number of modes is determined by including all of the lower modes that make the cumulative modal mass participation factor add up at least to 90% of the total seismic mass of the structure at hand.
3. Calculate distribution of the equivalent lateral forces consistent with the maximum story drifts.
4. Perform the pushover analysis in a single stage by the use of the equivalent lateral forces with a distribution calculated in the previous step.

The above steps are described in detail in the following subsections.

### 2.1 Calculation of the maximum story drifts

Under earthquake ground motions, the lateral displacement of the  $i$ -th story in the  $j$ -th mode for a rigid diaphragm, called  $u_{ij}$ , is calculated using Eq. (1):

$$u_{ij} = \phi_{ij}y_j \quad (1)$$

For a rigid diaphragm assumption, the in-plane motion of every diaphragm only includes two perpendicular horizontal displacements and a torsional rotation about the vertical axis. Therefore, accounting only for translational components of the ground motion,  $\phi_{ij}$  will be the element of the  $j$ -th mode shape vector corresponding to the horizontal motion of the  $i$ -th story parallel to the ground motion direction, and  $y_j$  is its corresponding modal response.  $y_j$  is determined using Eq. (2):

$$y_j = \Gamma_j S_{dj} \quad (2)$$

where  $\Gamma_j$  and  $S_{dj}$  are the modal contribution factor and the spectral displacement of the  $j$ -th mode, respectively, determined using Eqs. (3) and (4):

$$\Gamma_j = \frac{L_j}{M_j} \quad (3)$$

$$S_{aj} = \left( \frac{T_j^2}{4\pi^2} \right) S_{aj} \quad (4)$$

in which  $T_j$  and  $S_{aj}$  are the  $j$ -th mode period and spectral acceleration, respectively, and  $M_j$  and  $L_j$  are calculated from Eqs. (5) and (6):

$$M_j = \phi_j^T M \phi_j \quad (5)$$

$$L_j = \phi_j^T M r \quad (6)$$

where  $\phi_j$  is the  $j$ -th mode shape vector,  $M$  is the mass matrix, and  $r$  is an influence vector with its elements being all zero except the ones corresponding to the structure's horizontal degrees of freedom parallel to the ground motion.

Substitution of Eqs. (2–4) in Eq. (1) results in:

$$u_{ij} = \bar{u}_{ij} S_{aj}, \quad \bar{u}_{ij} = \phi_{ij} \Gamma_j \left( \frac{T_j^2}{4\pi^2} \right) \quad (7)$$

The modal story drift,  $d_{ij}$ , is calculated by deducting the lateral displacements of consecutive stories as follows:

$$d_{ij} = u_{ij} - u_{i-1j} \quad (8)$$

or, using Eq. (7):

$$d_{ij} = \bar{\phi}_{ij} \Gamma_j \left( \frac{T_j^2}{4\pi^2} \right) S_{aj}, \quad \bar{\phi}_{ij} = \phi_{ij} - \phi_{i-1j} \quad (9)$$

Equation (8) can also be written as:

$$d_{ij} = \bar{d}_{ij} S_{aj}, \quad \bar{d}_{ij} = \bar{\phi}_{ij} \Gamma_j \left( \frac{T_j^2}{4\pi^2} \right) \quad (10a)$$

$$d_{ij} = \bar{d}_{ij} S_{dj}, \quad \bar{d}_{ij} = \bar{\phi}_{ij} \Gamma_j \quad (10b)$$

where  $S_{dj}$  is the  $j$ -th mode spectral displacement.

Therefore, the  $i$ -th story drift in the  $j$ -th mode is calculated using Eqs. (10a, 10b).

## 2.2 Determination of the maximum story drift

The maximum drift of the  $i$ -th story,  $d_i$ , has to be calculated by combining the modal maxima in some way. The conventional method is using one of the well-known modal combination rules such as SRSS or CQC. The severe drawback to the mentioned methods is that by using them, signs of the modal responses are lost. Therefore, they might be good only for design, not analysis.

In this study, the maximum story drifts in each mode,  $d_{ij}$ , are first modified using a modification factor,  $\alpha_{ij}$ , and then combined to result in the absolute maximum story drift,  $d_i$ , as follows:

$$d_i = \sum_{j=1}^n \alpha_{ij} d_{ij} \tag{11}$$

where  $n$  is number of the desired modes.

As seen, the proposed summation keeps the signs of the modal responses. The modification factor  $\alpha_{ij}$  is used to account for the fact that the modal maxima do not occur at the same time and thus are not directly additive.

By resorting to the physics of the problem, the following alternative formulas are examined for  $\alpha_{ij}$ :

$$\alpha_{ij} = \left| \frac{\bar{D}_{ij}}{\sum_{j=1}^n \bar{D}_{ij}} \right|, \quad \bar{D}_{ij} = \bar{\phi}_{ij} \Gamma_j \tag{12}$$

$$\alpha_{ij} = \left| \frac{\bar{D}_{ij}}{\sum_{j=1}^n \bar{D}_{ij}} \right|, \quad \bar{D}_{ij} = \bar{\phi}_{ij} \Gamma_j \left( \frac{T_j^2}{4\pi^2} \right) \tag{13}$$

$$\alpha_{ij} = \left| \frac{\bar{D}_{ij}}{\sqrt{\sum_{j=1}^n \bar{D}_{ij}^2}} \right|, \quad \bar{D}_{ij} = \bar{\phi}_{ij} \Gamma_j \left( \frac{T_j^2}{4\pi^2} \right) S_{aj} \tag{14}$$

$$\alpha_{ij} = \alpha_j = \left| \frac{D_{Nj}}{\sum_{j=1}^n D_{Nj}} \right|, \quad D_{Nj} = \phi_{Nj} \Gamma_j \tag{15}$$

$$\alpha_{ij} = \alpha_j = \left| \frac{D_{Nj}}{\sum_{j=1}^n D_{Nj}} \right|, \quad D_{Nj} = \phi_{Nj} \Gamma_j \left( \frac{T_j^2}{4\pi^2} \right) \tag{16}$$

$$\alpha_{ij} = \alpha_j = \left| \frac{D_{Nj}}{\sqrt{\sum_{j=1}^n D_{Nj}^2}} \right|, \quad D_{Nj} = \phi_{Nj} \Gamma_j \left( \frac{T_j^2}{4\pi^2} \right) S_{aj} \tag{17}$$

In Eqs. (15–17),  $N$  is number of stories and  $\phi_{Nj}$  is the element of the  $j$ -th mode shape corresponding to the horizontal displacement at the roof parallel to the ground motion.

As observed, in Eqs. (12–14) a different modification factor is determined for each story in each mode. But, in Eqs. (15–17), a unique modification factor is calculated in each mode for all stories. In Eqs. (12) and (13)  $\alpha_{ij}$  varies as the weight of  $\bar{D}_{ij}$ , i.e. ratio of  $\bar{D}_{ij}$  to sum of  $\bar{D}_{ij}$ 's. In Eq. (12),  $\bar{D}_{ij}$  is taken to be the coefficient, or influence factor, of  $S_{aj}$  in Eq. (10b), while in Eq. (13),  $\bar{D}_{ij}$  is assumed to be the influence factor of  $S_{aj}$  in Eq. (10a). In Eq. (14),  $\bar{D}_{ij}$  is taken to be the  $i$ -th story drift at the  $j$ -th mode itself; therefore, its weight is calculated by dividing it to the total story drift that is calculated using the SRSS rule.

Equations (15–17) follow the same path but instead of the story responses here the weight is given to the response at the roof only, called the target response in the

conventional pushover analysis (CPA). Moreover, opposite to Eqs. (12, 13, 15 and 16),  $\alpha_{ij}$  is always less than unity in Eqs. (14) and (17).

The inherent approximation in Sects. 2.1 and 2.2 is use of elastic stiffness of structure all the way to computing its maximum story drifts. This strategy has been selected deliberately to retain the simplicity of the proposed pushover procedure. However, this should not have severe consequences since it has been already known that the linear and nonlinear drift responses are similar for buildings having fundamental periods larger than 0.5 s. Use of elastic dynamic characteristics in an inelastic static analysis (pushover) method is common. It is used in the conventional as well as the modal pushover procedures, to name just the more pronounced methods.

### 2.3 Calculation of distribution of the lateral forces

In a more involved procedure, distribution of lateral forces which produce the story drifts  $d_i$  ( $i = 1, \dots, N$ ) calculated by Eq. (11), should change with the plastically decreasing shear stiffness of each story. This fact is not in line with the goal of simplicity in pushover analysis. Therefore, one has to make logical simplifying assumptions at this step, as follows.

Two alternative assumptions are examined for calculating the distribution of the equivalent lateral forces,  $\bar{f}_i$ . First, the lateral forces are determined as the difference between the elastic story shears of the successive stories. These are then normalized to the base shear as:

$$\bar{f}_i = \frac{K_i d_i - K_{i+1} d_{i+1}}{K_1 d_1} \quad (18)$$

Second, the lateral forces distribution is taken to be similar to that of lateral displacements normalized to the displacement of roof as follows:

$$\bar{f}_i = \frac{\sum_{m=1}^i d_m}{\sum_{m=1}^N d_m} \quad (19)$$

Considering six alternatives for calculation of the total story drift  $d_i$  (Eqs. 11–17) and two alternatives for determining distribution of the equivalent lateral forces  $\bar{f}_i$  (Eqs. 18 and 19), totally 12 cases has to be considered for response calculation using DPA and comparison with CPA, MPA and NTA.

## 3 Buildings considered

Since the three dimensional DPA method is being proposed to extend the pushover analysis to taller irregular buildings, 10, 15, 20 and 30-story moment frame structures are considered. To have a same basis for comparison, the buildings are assumed to be symmetrical in stiffness, meaning that the center of stiffness is located at the center of plan (or area) at each story. To make eccentricity later in the nonlinear analysis, only the center of mass will be changed. This way, variety of live load location is simulated. Therefore, no eccentricity is assumed when designing the structures. Of course, the developed pushover procedure is independent of the type of torsional eccentricity.

The buildings under study are steel special moment frames. The story plan is identical for all stories and buildings. It has three bays in each direction and the bay spans are identically 5 m (Fig. 1). It should be mentioned that in the case of concrete structures, the effective section of each member should be used in the analysis.

The story heights are equally 3.2 m. The buildings rest on a firm soil, i.e. the soil type C according to ASCE7-10 (2010). Seismicity of the area is assumed to be very high represented by the design spectrum shown in Fig. 2. The total dead load including partitions is taken to be  $6 \text{ kN/m}^2$  and the live load is  $2 \text{ kN/m}^2$ . The buildings are calculated according to ASCE7-10 (2010) and AISC360-10 (2010).

Box and I sections are used for the columns and girders, respectively, as shown in Table 1. The dynamic characteristics of the first three modes of the buildings are shown in Table 2. The mode shapes of the first, second and third modes are shown in Fig. 3.

#### 4 Nonlinear modeling of the structures

For nonlinear dynamic analysis, the structures are modeled by OpenSees software (Mazzone et al. 2006). The nonlinear bending action is assumed to be potentially concentrated at the ends of the beams and columns. Such sections are assumed to be composed of longitudinal steel fibers. The nonlinear behavior is a resultant of one-dimensional nonlinear deformation of fibers. Since the dynamic analysis includes several reversals of loading at each section, the nonlinear stress–strain model of the fibers should realistically include the cyclic behavior of steel. The Steel02 material of OpenSees can take care of loading reversals by a smooth transition between the elastic and inelastic regions and by accounting for the Bauschinger effect. The stress–strain behavior of Steel02 material is shown in Fig. 4.

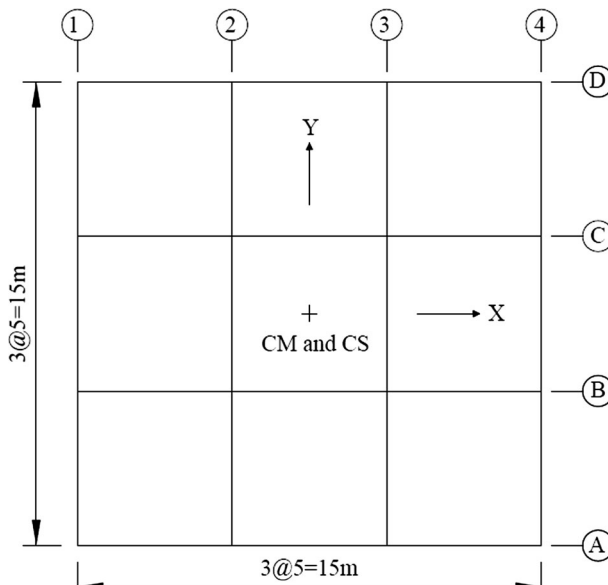


**Fig. 1** Typical story plan

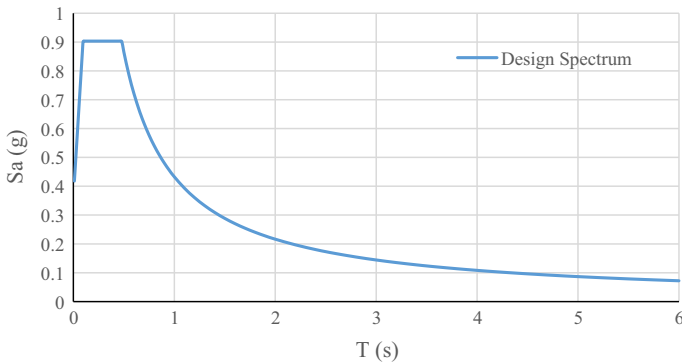


**Fig. 2** The design spectrum

## 5 The ground motions

For consistency of the analysis results, the selection criteria of the ground motions are taken as follows. The soil type C (ASCE7-10) that is a medium soil is assumed for the location of the recordings. The fault distance is taken to be intermediate (20–50 km) and the earthquake magnitude is 6–8 Richters. The PEER database is consulted for ground motion selection (PEER Ground Motion Database 2016).

Use of the above criteria results in finding 61 earthquake records in the database as of July 2016. For screening, in each earthquake only a single recording station with the largest peak ground acceleration (PGA) is retained. Between the remained records, 10 earthquakes with the scale factors nearest to unity are retained because of their more consistency with the design spectrum.

Finally, the original records of the selected earthquakes are scaled such that, according to ASCE7-10 (2010), the averaged response spectrum is not lower than the design spectrum nowhere in the range of  $0.2 T$ – $1.5 T$  where  $T$  is the fundamental period of the building under study. The scale factor appears to be 1.94, 1.73, 1.47 and 1.47 for 10, 15, 20 and 30-story buildings, respectively. Table 3 shows the characteristics of the selected earthquakes.

For instance, the average response spectrum is shown in Fig. 5 before and after scaling for the 20-story building against the design spectrum.

## 6 The analysis results

### 6.1 Time history analysis

Nonlinear dynamic analysis of the buildings is performed under the selected records. The response parameters to be calculated are maximum lateral displacements of stories that happen at the corner of plan at the side of the mass center (points A and CM in Fig. 6, respectively), maximum story shears, and maximum plastic hinge rotations of stories. For calculation of the latter parameter, time histories of the plastic hinge rotations of the beams and columns of each story are added at each time step after removing signs of the numbers and the maximum value is extracted at each story. The perpendicular horizontal



**Table 1** Section properties

Story	10-story		15-story		20-story		30-story	
	Beams	Columns	Beams	Columns	Beams	Columns	Beams	Columns
1	IPE400	BOX350	IPE450	BOX450	IPE450	BOX500	IPE550	BOX550
2	IPE400	BOX350	IPE450	BOX450	IPE450	BOX500	IPE550	BOX550
3	IPE400	BOX350	IPE450	BOX450	IPE450	BOX500	IPE550	BOX550
4	IPE360	BOX350	IPE450	BOX400	IPE450	BOX500	IPE550	BOX500
5	IPE360	BOX350	IPE450	BOX400	IPE450	BOX500	IPE550	BOX500
6	IPE360	BOX350	IPE450	BOX400	IPE450	BOX500	IPE550	BOX500
7	IPE330	BOX350	IPE400	BOX350	IPE450	BOX450	IPE550	BOX450
8	IPE330	BOX350	IPE400	BOX350	IPE450	BOX450	IPE550	BOX450
9	IPE330	BOX350	IPE400	BOX350	IPE450	BOX450	IPE550	BOX450
10	IPE330	BOX350	IPE400	BOX350	IPE450	BOX450	IPE550	BOX400
11			IPE400	BOX350	IPE400	BOX400	IPE550	BOX400
12			IPE400	BOX350	IPE400	BOX400	IPE550	BOX400
13			IPE360	BOX350	IPE400	BOX400	IPE550	BOX400
14			IPE360	BOX350	IPE400	BOX350	IPE550	BOX400
15			IPE360	BOX350	IPE400	BOX350	IPE550	BOX400
16					IPE400	BOX350	IPE500	BOX400
17					IPE360	BOX350	IPE500	BOX400
18					IPE360	BOX350	IPE500	BOX400
19					IPE360	BOX350	IPE500	BOX400
20					IPE360	BOX350	IPE500	BOX400
21							IPE500	BOX400
22							IPE500	BOX400
23							IPE500	BOX400
24							IPE500	BOX400
25							IPE500	BOX350
26							IPE450	BOX350
27							IPE450	BOX350
28							IPE450	BOX350
29							IPE450	BOX350
30							IPE450	BOX350

components of ground motions are applied to the models simultaneously in x and y-directions (Fig. 6).

The above calculations are implemented for 0, 5, 10, 15, and 30% eccentricity ratios. The eccentricity is constructed by displacing the center of mass from the center of plan (or the stiffness center) equally in x and y directions at a value normalized to the plan dimension by the above amounts. Although a 30% eccentricity seems to be rare, it is also included as an extreme case.

**Table 2** Dynamic characteristics of the buildings

No. of stories	First mode				Second mode				Third mode			
	T	$\Gamma$	$S_a$	PF*	T	$\Gamma$	$S_a$	PF*	T	$\Gamma$	$S_a$	PF*
10	1.94	1.34	0.22	0.76	0.65	-0.53	0.67	0.12	0.35	0.31	0.91	0.05
15	2.41	1.35	0.18	0.75	0.83	-0.56	0.52	0.12	0.48	0.33	0.90	0.04
20	3.11	1.37	0.14	0.74	1.10	-0.58	0.39	0.13	0.63	0.33	0.69	0.04
30	3.94	1.41	0.11	0.72	1.31	-0.62	0.33	0.14	0.74	0.34	0.58	0.04

\*PF Mass participation factor

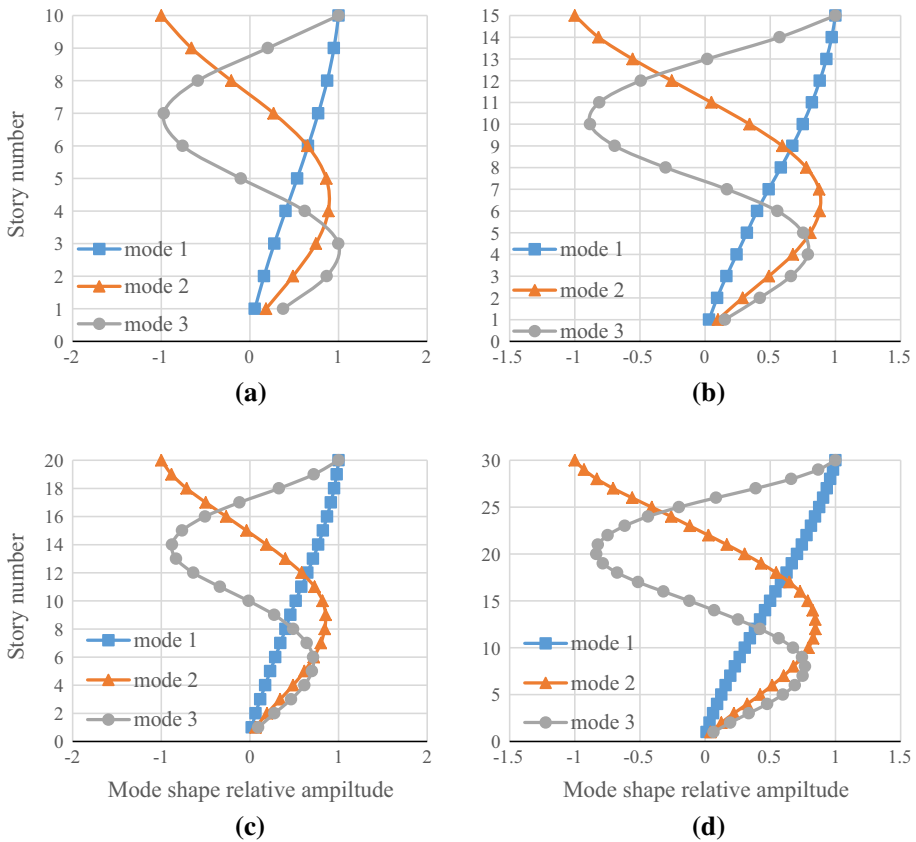


**Fig. 3** Natural mode shapes. **a** 10-story; **b** 15-story; **c** 20-story; **d** 30-story building

### 6.2 Pushover analysis

For comparison, in addition to the methods proposed in this study, results for the conventional pushover analysis (CPA) and modal pushover analysis (MPA) are also presented.

In all of the pushover procedures, the buildings are pushed by a certain distribution of lateral forces up to the point where the center of mass of the roof is displaced equal to a

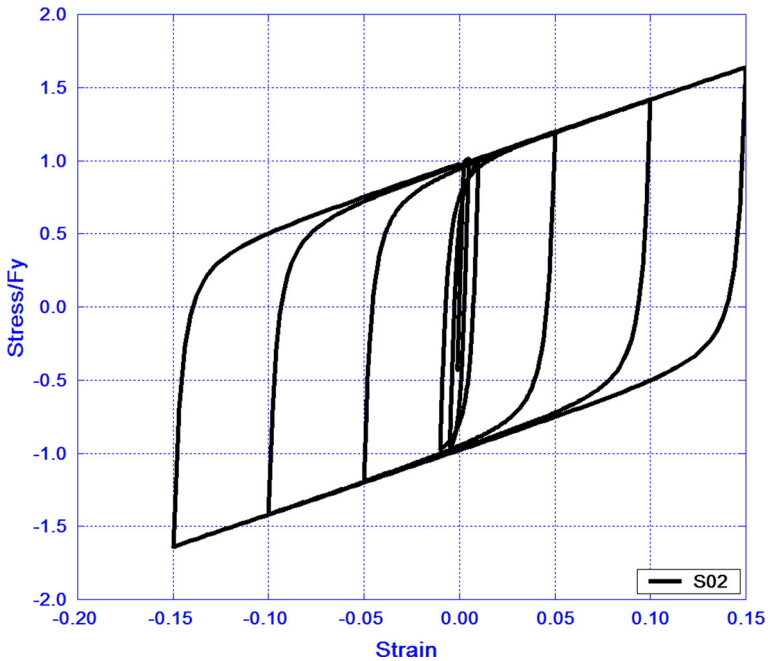


**Fig. 4** The stress–strain behavior of the Steel02 material

**Table 3** Characteristics of the earthquakes

Order	EQ. name	PEER no.	Distance (km)	Magnitude (Richter)	Year	PGA (g)
1	San Fernando	88	24.87	6.61	1971	0.22
2	Irpinia, Italy	286	21.26	6.90	1980	0.13
3	Loma Prieta	755	20.34	6.93	1989	0.51
4	Chi–Chi, Taiwan	1484	26.31	7.62	1999	0.33
5	Cape Mendocino	3750	25.91	7.01	1992	0.37
6	Landers	3757	26.95	7.28	1992	0.20
7	Tottori, Japan	3932	26.51	6.61	2000	0.53
8	Chuetsu-Oki, Japan	4882	23.44	6.80	2007	0.49
9	Iwate, Japan	5663	20.18	6.90	2008	1.04
10	Darfield, New Zealand	6915	24.47	7.00	2010	0.86

value called the target displacement. It is an amount expected to occur in the design earthquake. In ASCE41-13 [16], a procedure, called the displacement coefficients method, has been given for calculation of the target displacement. In this procedure, first the spectral displacement (at the mass center of the building) is determined. It is then converted to the lateral displacement of roof using the first mode characteristics of the building. It is also somewhat magnified for the effects of nonlinear behavior and the P-delta phenomenon. The target displacements are proved to be 36.85, 45.4, 59.4, and 79.5 cm for the 10, 15, 20, and 30-story buildings under study.

**Fig. 5** The scaled and non-scaled average response spectra against the design spectrum for the 20-story building

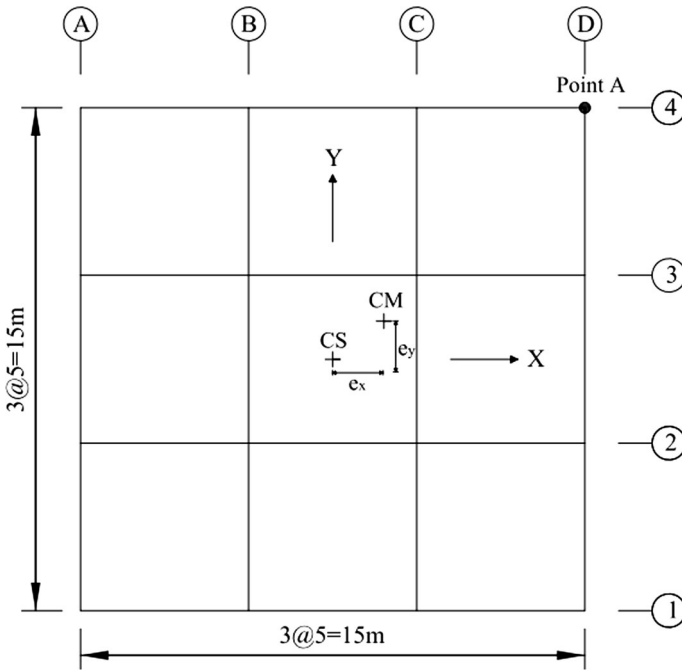
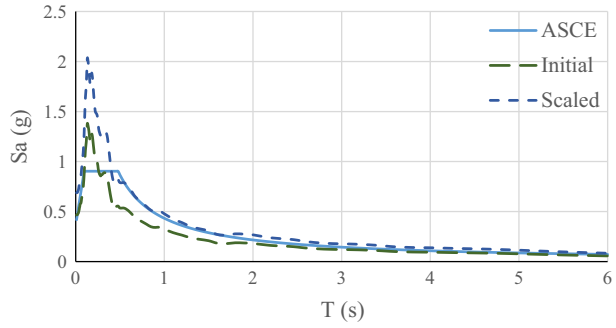


**Fig. 6** Eccentricity in the plan

The CPA procedure in this paper is the one introduced in ASCE41-13 (2014). In this method, distribution of the lateral forces is taken to be the same as the fundamental mode shape of the building. In MPA, according to Chopra and Goel (2000), the target displacement and lateral load distribution are calculated similar to CPA but for each mode separately. The response results are then combined using one of the modal combination rules.

In Sect. 2 of this paper, a drift pushover analysis (DPA) procedure has been introduced in 12 variations. Distribution of the equivalent lateral forces that produces the drifts given in Eq. (11) is taken to be calculated from Eqs. (18) or (19) where the modification factor

$\alpha_{ij}$  is determined using one of the approaches given in Eqs. (12)–(17). To distinguish between the different DPA procedures, they are named as DPA1 to DPA6 when Eqs. (12)–(17) are used with Eq. (18), respectively, and as DPA7 to DPA12 when they are used respectively with Eq. (19).

In all, results of the pushover analysis, for the same response parameters as described in Sect. 6.1, will be presented and compared for CPA, MPA, and DPA1–DPA12.

Two series of results are discussed. First, for each building, deviation of the response parameters from those of NTA are presented as resultant RMS error values for different eccentricities in a number of tables. The resultant RMS error percent is the resultant of error all over a structure as defined in Eq. (20):

$$RMS(\%) = 100 \sqrt{\frac{1}{N} \sum_{i=1}^N \left( \frac{X_{iD} - X_{iP}}{X_{iD}} \right)^2} \tag{20}$$

where  $X_{iD}$  and  $X_{iP}$  are values of the story response parameter according to the nonlinear time history and pushover analysis, respectively, and N is number of stories.

In the second series, distributions of RMS of the response parameters are presented comparatively as graphs drawn along height of the buildings for DPA, MPA, and CPA procedures only for a 15% eccentricity as an example for the torsional cases. In this case, the RMS value for the  $i$ -th story is equal to the value of the quantity between parentheses in Eq. (20).

One important fact regarding the PHRs should be noticed. It is well known that plastic hinges usually are more concentrated in the lower half of frame buildings. Sometimes, there are some upper stories that do not experience nonlinear behavior at all. Therefore, the following approach is taken to deal with the RMS of the PHRs. In each building, first the story having the maximum PHR is identified. Then all of the story PHRs are normalized to the maximum value. In the upper stories where this normalized value falls below 0.05, i.e. 5% of the maximum value, the PHRs are neglected and no RMS is calculated for the PHRs there.

### 6.3 Resultant RMS of the pushover procedures

In Tables 4, 5, 6, 7, 8, 9, 10, 11, 12, 13, 14 and 15, the RMS values are given for each building and response parameter for different values of eccentricity. They are calculated using Eq. (20). For better display, the cases of DPA where the RMS is smaller than that of MPA (referenced as an enhanced pushover method being superior in accuracy with regard to CPA) are indicated in italics.

**Table 4** The RMS errors (%) with respect to NTA for the corner displacement of plan, 10-story building

Ecc. (%)	Calculation method (MPA, CPA, DPAn where n = 1–12)													
	MPA	CPA	1	2	3	4	5	6	7	8	9	10	11	12
0	10.8	12.4	73.8	22.1	<i>10.2</i>	<i>6.5</i>	<i>4.5</i>	8.6	75.5	30.3	62.9	49.9	49.9	49.9
5	11.1	12.7	73.9	22.3	<i>9.2</i>	<i>5.7</i>	<i>4.5</i>	9.0	75.8	30.4	62.5	49.6	49.6	49.6
10	11.9	13.6	73.8	22.8	<i>7.9</i>	<i>4.6</i>	<i>5.3</i>	9.9	76.2	29.2	60.2	47.7	47.7	47.7
15	13.1	14.9	73.8	23.8	<i>5.9</i>	<i>3.2</i>	<i>7.0</i>	<i>11.3</i>	76.6	27.3	56.9	44.9	44.9	44.9
30	22.4	24.4	74.6	31.3	<i>9.8</i>	<i>12.6</i>	<i>19.2</i>	<i>21.4</i>	78.3	20.6	44.7	34.4	34.4	34.4

**Table 5** The RMS errors (%) with respect to NTA for the corner displacement of plan, 15-story building

Ecc. (%)	Calculation method (MPA, CPA, DPAn where n = 1–12)													
	MPA	CPA	1	2	3	4	5	6	7	8	9	10	11	12
0	8.1	7.1	52.7	20.4	20.7	20.3	2.8	5.9	47.9	46.1	82.4	65.2	65.2	65.2
5	8.5	7.5	53.9	20.5	19.2	18.8	3.5	5.7	48.3	44.8	80.4	63.6	63.6	63.6
10	8.8	7.8	54.4	20.7	17.2	16.7	3.0	5.2	48.7	42.8	77.3	61.1	61.1	61.1
15	8.8	8.0	54.2	20.7	15.1	14.7	1.5	4.2	48.9	40.9	74.1	58.7	58.7	58.7
30	10.6	10.8	52.9	21.4	13.0	12.5	6.1	7.0	49.0	37.8	70.0	56.6	56.6	56.6

**Table 6** The RMS errors (%) with respect to NTA for the corner displacement of plan, 20-story building

Ecc. (%)	Calculation method (MPA, CPA, DPAn where n = 1–12)													
	MPA	CPA	1	2	3	4	5	6	7	8	9	10	11	12
0	22.5	20.0	49.1	17.3	43.8	42.8	19.9	25.5	38.4	63.0	96.6	81.9	81.9	81.9
5	23.6	19.9	47.8	17.1	42.7	41.8	19.9	25.2	38.1	62.2	96.2	81.2	81.2	81.2
10	22.7	18.3	46.3	16.3	40.4	39.5	18.4	23.3	37.9	60.4	94.1	79.4	79.4	79.4
15	20.8	16.4	45.5	15.4	38.4	37.2	16.6	21.1	37.7	58.5	91.6	77.5	77.5	77.5
30	13.3	10.6	46.4	16.6	29.7	27.1	11.5	12.9	38.9	47.2	78.7	67.2	67.2	67.2

**Table 7** The RMS errors (%) with respect to NTA for the corner displacement of plan, 30-story building

Ecc. (%)	Calculation method (MPA, CPA, DPAn where n = 1–12)													
	MPA	CPA	1	2	3	4	5	6	7	8	9	10	11	12
0	14.1	17.9	64.6	15.7	45.6	45.6	10.0	21.6	52.8	75.2	121.2	96.5	96.5	96.5
5	15.5	19.6	66.5	15.3	45.9	45.8	12.4	22.7	53.6	75.1	120.1	96.0	96.0	96.0
10	14.3	18.5	66.9	14.6	44.4	44.4	12.5	21.3	53.8	73.9	117.7	94.5	94.5	94.5
15	9.4	13.8	65.0	14.3	39.1	39.3	9.1	16.1	53.2	68.9	110.9	88.9	88.9	88.9
30	5.9	6.0	60.0	19.1	21.9	22.6	2.5	2.5	52.1	51.5	90.5	71.2	71.2	71.2

Looking through Tables 4, 5, 6, 7, 8, 9, 10, 11, 12, 13, 14 and 15 reveals two important points. First, there are DPA procedures for all of the buildings studied, all of the response parameters, and all of the eccentricity ratios, that perform better and have more accuracy with respect to MPA. Second, while number of better DPA procedures decreases for taller buildings, DPA5 always is the most accurate within the studied pushover procedures. Distribution of the equivalent lateral forces in DPA5 is shown in Fig. 7 Here, the first three modes are included, i.e.,  $n = 3$  in Eqs. (11) and (16).

As stated in Sect. 2, in DPA5 the modal drift modification factor  $\alpha_{ij}$  is calculated from Eq. (16). It is then used in Eqs. (11) and (18) to calculate the story drifts and distribution of lateral forces, respectively. According to Eq. (16), as explained in Sect. 2,  $\alpha_{ij}$  is assumed to be proportional to the influence factor of the spectral acceleration (not displacement) and the roof displacement in each mode. Since the lateral forces vary also with the response

**Table 8** The RMS errors (%) with respect to NTA for the story shear, 10-story building

Ecc. (%)	Calculation method (MPA, CPA, DPAn where n = 1–12)													
	MPA	CPA	1	2	3	4	5	6	7	8	9	10	11	12
0	10.8	32.0	184.6	11.8	34.6	18.8	8.6	10.4	177.3	27.9	41.1	41.3	41.3	41.3
5	10.6	31.9	184.9	11.7	34.6	18.8	8.5	10.3	177.4	28.0	41.1	41.3	41.3	41.3
10	9.9	31.7	184.2	11.6	34.6	18.8	8.5	10.3	176.6	28.1	41.3	41.4	41.4	41.4
15	8.8	31.7	183.7	11.6	34.5	18.7	8.6	10.3	176.1	28.1	41.1	41.3	41.3	41.3
30	8.8	34.7	176.5	14.7	34.6	19.7	8.6	13.1	168.8	28.1	40.6	40.9	40.9	40.9

**Table 9** The RMS errors (%) with respect to NTA for the story shear, 15-story building

Ecc. (%)	Calculation method (MPA, CPA, DPAn where n = 1–12)													
	MPA	CPA	1	2	3	4	5	6	7	8	9	10	11	12
0	19.7	27.9	108.9	12.7	33.2	20.4	9.7	11.5	96.5	33.2	42.6	42.2	42.2	42.2
5	19.7	27.7	108.7	12.7	33.1	20.3	9.7	11.5	96.3	33.3	42.6	42.1	42.1	42.1
10	19.5	27.3	108.0	12.6	32.9	20.1	9.6	11.2	95.5	33.3	42.5	42.0	42.0	42.0
15	17.4	27.4	106.8	12.5	32.9	20.2	9.4	11.2	94.3	33.0	42.6	42.1	42.1	42.1
30	10.8	32.0	102.0	13.5	33.7	21.5	11.3	13.2	88.9	32.7	42.4	42.3	42.3	42.3

**Table 10** The RMS errors (%) with respect to NTA for the story shear, 20-story building

Ecc. (%)	Calculation method (MPA, CPA, DPAn where n = 1–12)													
	MPA	CPA	1	2	3	4	5	6	7	8	9	10	11	12
0	27.9	22.0	101.6	19.1	33.0	23.7	17.2	17.6	83.7	37.4	45.0	44.1	44.1	44.1
5	27.8	21.9	101.8	19.4	33.0	23.8	17.4	17.8	83.8	37.6	45.1	44.2	44.2	44.2
10	26.7	21.8	101.5	19.5	33.0	23.7	17.4	17.7	83.5	37.6	45.1	44.1	44.1	44.1
15	24.0	22.2	100.8	19.1	32.6	23.1	16.8	17.1	82.4	37.1	44.6	43.7	43.7	43.7
30	12.3	25.9	100.8	16.1	31.6	21.1	13.4	14.2	80.1	34.6	42.3	41.8	41.8	41.8

acceleration, such a result more or less is expectable. Performance of DPA5 along building height is discussed in the next section.

#### 6.4 Height-wise distribution of RMS for the pushover procedures

Figures 8, 9, 10, 11, 12, 13, 14, 15, 16, 17, 18 and 19 exhibit how the RMS values of the response parameters change along height of the buildings for CPA, MPA, and DPA5. The later method was shown to be the superior DPA procedure in the previous section.

In Figs. 8, 9, 10, 11, 12, 13, 14, 15, 16, 17, 18 and 19 it is very interesting to note that in most cases DPA5 performs better than CPA and MPA along height of the buildings too.

**Table 11** The RMS errors (%) with respect to NTA for the story shear, 30-story building

Ecc. (%)	Calculation method (MPA, CPA, DPAn where n = 1–12)													
	MPA	CPA	1	2	3	4	5	6	7	8	9	10	11	12
0	23.5	19.3	95.9	23.6	26.2	20.4	18.5	16.6	91.0	32.4	43.5	41.7	41.7	41.7
5	23.1	19.3	95.9	23.4	26.3	20.6	18.4	16.6	91.0	32.5	43.6	41.8	41.8	41.8
10	21.5	19.6	96.1	22.1	26.4	20.7	17.8	16.3	90.8	32.6	43.7	41.9	41.9	41.9
15	18.9	20.2	95.6	19.9	26.0	20.4	16.5	15.4	89.9	32.7	43.7	41.8	41.8	41.8
30	9.3	25.5	93.3	12.7	24.9	19.1	9.4	9.9	86.1	32.2	43.3	41.5	41.5	41.5

**Table 12** The RMS errors (%) with respect to NTA for the story plastic hinge rotation, 10-story building

Ecc. (%)	Calculation method(MPA, CPA, DPAn where n = 1–12)													
	MPA	CPA	1	2	3	4	5	6	7	8	9	10	11	12
0	57.4	63.6	434.4	45.2	56.5	53.4	43.8	45.9	261.8	70.9	98.7	87.3	87.3	87.3
5	55.8	59.0	377.2	42.2	55.5	51.2	40.4	43.3	236.1	67.8	92.6	83.0	83.0	83.0
10	55.0	56.4	332.8	40.5	55.0	49.9	38.5	41.2	218.3	65.2	87.1	79.1	79.1	79.1
15	55.0	55.8	295.3	40.2	55.0	49.7	38.4	40.7	203.1	63.4	83.1	76.3	76.3	76.3
30	57.3	62.3	244.8	46.0	58.6	54.0	45.4	47.0	182.4	63.2	77.6	73.1	73.1	73.1

While in the lower half of the building height accuracy of DPA5 is generally similar to or better than MPA, in the upper half it performs almost always better than MPA.

The RMS errors of DPA5 for story displacements in Tables 4, 5, 6, 7, 8, 9, 10, 11, 12, 13, 14 and 15 and Figs. 8, 9, 10, 11, 12, 13, 14, 15, 16, 17, 18 and 19, are everywhere smaller than 20%. This is sufficiently small for engineering purposes. For the case of story shears, the maximum resultant RMS errors of DPA5 (mentioned in the tables) are again less than 20% that is good. The maximum RMS error at a story (mentioned in the figures) reaches to about 40% for the two taller structures. This happens in the upper half of the buildings. Therefore, if it is desired that the story shears are estimated with smaller errors in any story (say with an RMS < 30%), DPA5 should be modified in this regard in the upper half of the taller buildings.

For story plastic hinge rotations, the maximum resultant RMS errors of DPA5 are 25–50% in different cases that is not too much compared to other existing methods. On the other hand, the maximum RMS error at a story can be as large as 80%. As appears in the figures, it can be large both for the short and tall buildings and can happen both in the lower and upper half of the structures. Therefore, it seems necessary to modify DPA5 for the total height of all buildings to give better estimates of story PHR values. However, due to the large number of plastic hinges in frames and variety of their rotations, the tolerable estimation error for the PHR's should be larger than the other response parameters. The acceptable resultant RMS error for PHR can be taken as 40% compared to 30% for shear and 20% for displacements.

A remedy for the mentioned issue is suggested in the next section.



**Table 13** The RMS errors (%) with respect to NTA for the story plastic hinge rotation, 15-story building

Ecc. (%)	Calculation method(MPA, CPA, DPAn where n = 1–12)													
	MPA	CPA	1	2	3	4	5	6	7	8	9	10	11	12
0	59.8	67.6	105.3	57.6	63.1	66.4	51.7	53.1	95.5	106.2	164.9	133.1	133.1	133.1
5	56.8	62.6	102.9	53.1	61.2	63.5	46.6	49.8	92.5	96.5	144.1	118.6	118.6	118.6
10	54.2	58.3	100.4	49.2	59.9	61.5	42.7	46.5	89.7	90.5	132.0	110.5	110.5	110.5
15	53.3	56.7	98.3	46.6	59.1	59.9	41.0	44.7	87.7	86.1	123.4	104.9	104.9	104.9
30	52.3	60.7	94.0	45.0	59.6	58.8	42.8	45.7	84.2	82.0	117.1	102.0	102.0	102.0

**Table 14** The RMS errors (%) with respect to NTA for the story plastic hinge rotation, 20-story building

Ecc. (%)	Calculation method (MPA, CPA, DPAn where n = 1–12)													
	MPA	CPA	1	2	3	4	5	6	7	8	9	10	11	12
0	47.2	56.2	177.2	59.6	81.0	85.2	41.9	51.6	194.6	135.0	214.3	171.5	171.5	171.5
5	42.5	49.0	165.0	54.3	78.3	81.6	36.2	47.1	174.6	126.8	196.3	159.7	159.7	159.7
10	39.2	43.2	156.7	49.4	75.6	77.8	31.4	42.7	164.4	120.5	183.3	151.2	151.2	151.2
15	35.3	39.3	155.7	46.4	73.9	74.7	25.7	37.9	162.2	118.4	179.7	149.4	149.4	149.4
30	38.9	45.3	165.2	34.9	63.3	60.3	23.9	31.7	135.5	95.4	143.9	123.4	123.4	123.4

**Table 15** The RMS errors (%) with respect to NTA for the story plastic hinge rotation, 30-story building

Ecc. (%)	Calculation method(MPA, CPA, DPAn where n = 1-12)													
	MPA	CPA	1	2	3	4	5	6	7	8	9	10	11	12
0	53.5	77.6	288.2	91.3	99.3	105.8	45.5	62.9	69.1	175.4	295.5	220.0	220.0	220.0
5	41.8	67.0	262.7	86.5	96.2	102.8	32.9	52.4	465.3	167.3	273.1	207.0	207.0	207.0
10	36.1	61.2	223.9	70.4	92.6	99.4	25.2	45.9	327.5	162.1	258.7	198.8	198.8	198.8
15	36.2	60.8	187.5	58.2	83.3	89.9	24.1	39.9	263.0	146.0	227.1	177.4	177.4	177.4
30	48.4	67.0	141.2	45.0	65.6	70.7	37.6	42.3	165.1	113.3	171.9	137.8	137.8	137.8

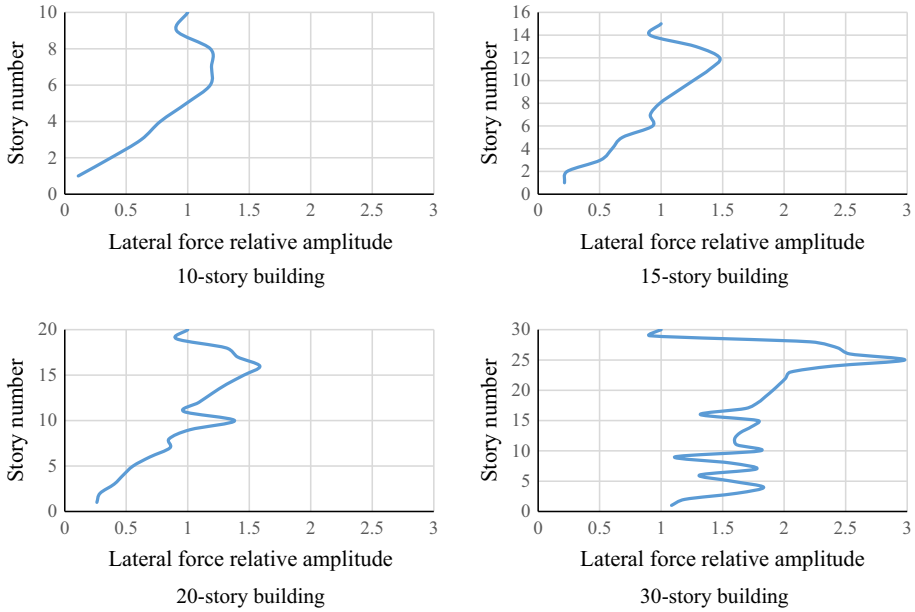


**Fig. 7** Distribution of equivalent lateral forces by combining the first three modes, DPA5

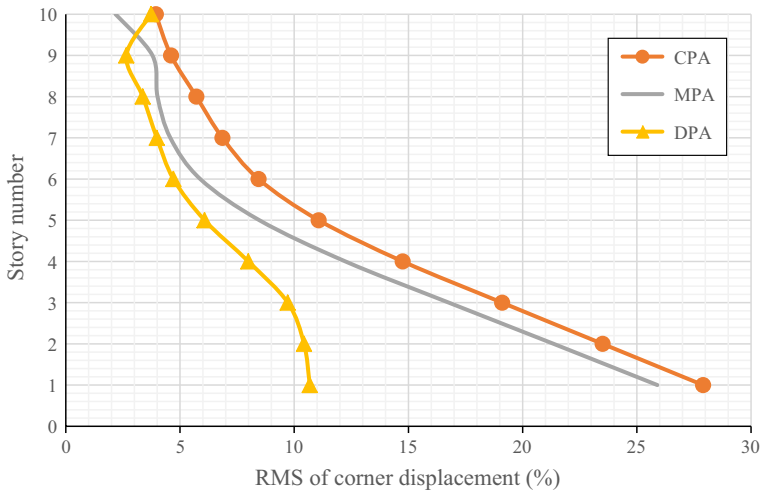


**Fig. 8** RMS values for a 15% eccentricity, 10-story building, corner displacement (point A in Fig. 6)

### 6.5 Reduction of RMS errors of DPA5

#### 6.5.1 Story shear estimation in the upper half stories of the taller buildings

The goal in this section is to reduce the resultant RMS error of DPA5 in estimating the story shears in the upper half stories of the 20 and 30-story buildings.

According to Eq. (11), the story shear is calculated as:

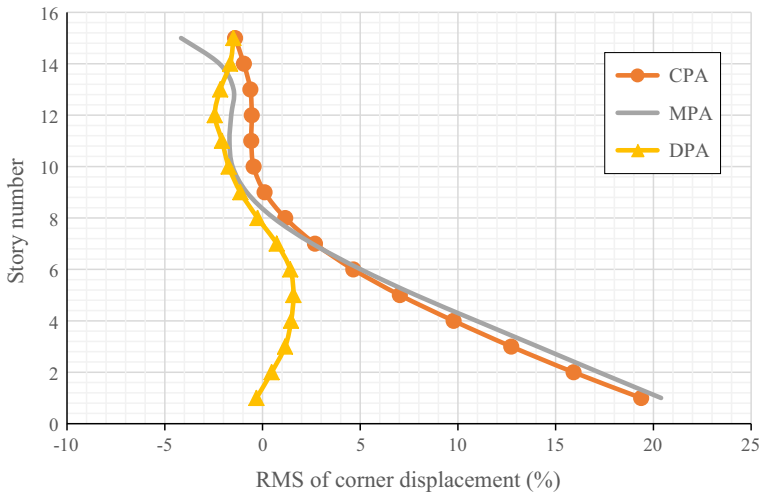


**Fig. 9** RMS values for a 15% eccentricity, 15-story building, corner displacement (point A in Fig. 6)

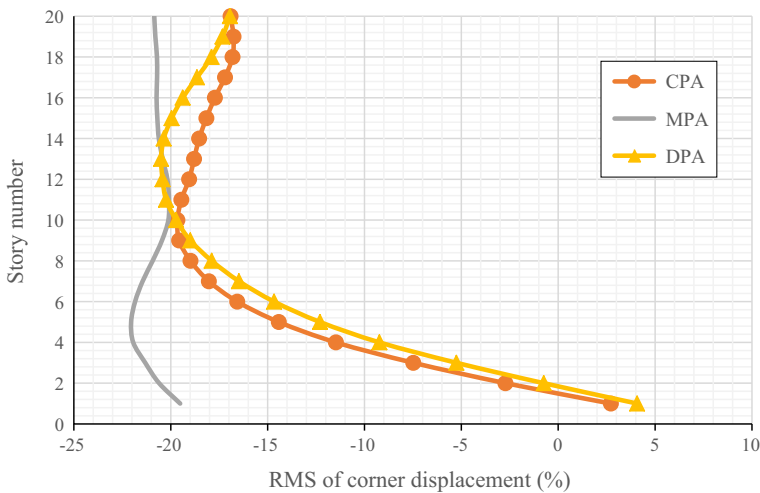


**Fig. 10** RMS values for a 15% eccentricity, 20-story building, corner displacement (point A in Fig. 6)

$$V_i = K_i \sum_{j=1}^n \alpha_j d_{ij} \tag{21}$$

in which  $\alpha_j$  is determined using Eq. (16). According to Eq. (16),  $\alpha_j$  is likely to be larger and smaller than unity for lower and higher modes, respectively. Therefore,  $\sum_{j=1}^n \alpha_j$  is always larger than unity. As observed in Figs. 14 and 15, the story shear estimated by DPA5 in the upper stories is generally larger than its exact value (because the story RMS, that is the term inside parentheses in Eq. 20, is negative). Therefore, it can be expected that by reducing  $V_i$ , RMS is also decreased. Then, it is decided to reduce the story shears in the upper half stories by dividing them by  $\sum_{j=1}^n \alpha_j$  as follows:

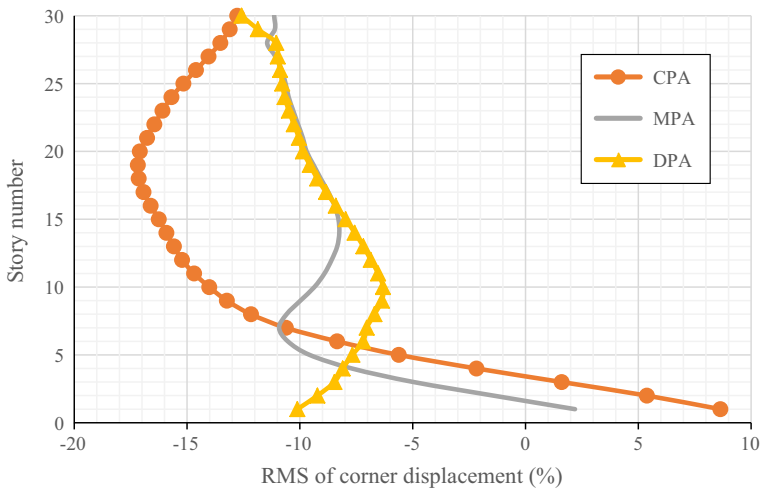


**Fig. 11** RMS values for a 15% eccentricity, 30-story building, corner displacement (point A in Fig. 6)

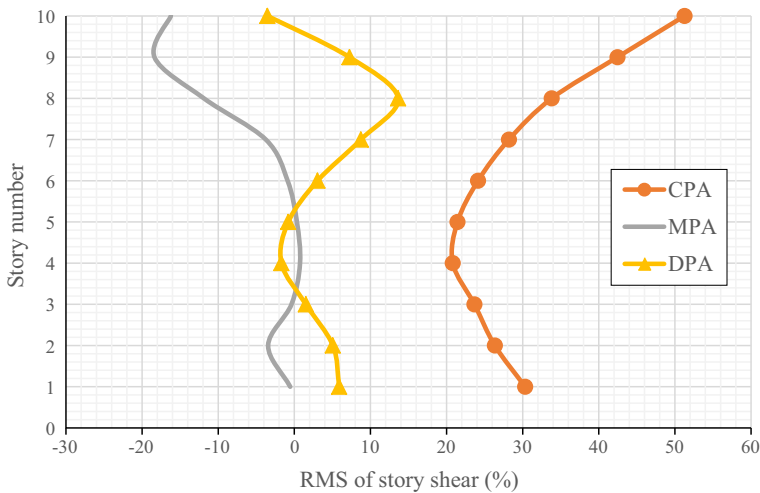


**Fig. 12** The story-wise RMS values for a 15% eccentricity, 10-story building, story shear

$$\bar{V}_i = \frac{V_i}{\sum_{j=1}^n \alpha_j} = K_i \frac{\sum_{j=1}^n \alpha_j d_{ij}}{\sum_{j=1}^n \alpha_j}, \quad i = [N/2], \dots, N, \quad n = 20 \text{ or } 30 \quad (22)$$

where  $[N/2]$  shows the integer part of  $N/2$  and  $\bar{V}_i$  is the modified value of  $V_i$  in the upper stories. Use of Eq. (22) is equivalent to calculating  $V_i$ 's using the weighted average of modal story drifts of the  $i$ -th story. Values of  $\alpha_j$  are given for the studied buildings in Table 16. In Table 17, it is shown that the above procedure has been successful in reducing the resultant RMS errors, as well as the maximum story RMS error, of DPA5 in estimating the story shears in the upper half of the taller buildings to values much smaller than those of the CPA and MPA procedures. This resultant is calculated using Eq. (20) by  $i = [N/2], \dots, N$ .

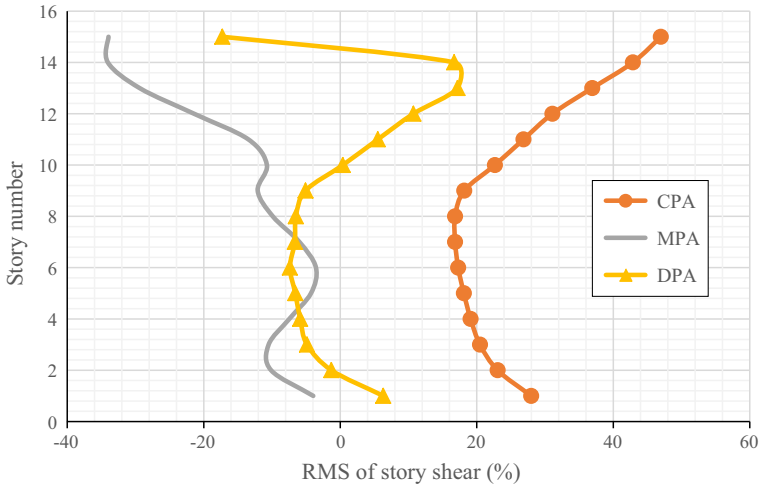


**Fig. 13** The story-wise RMS values for a 15% eccentricity, 15-story building, story shear

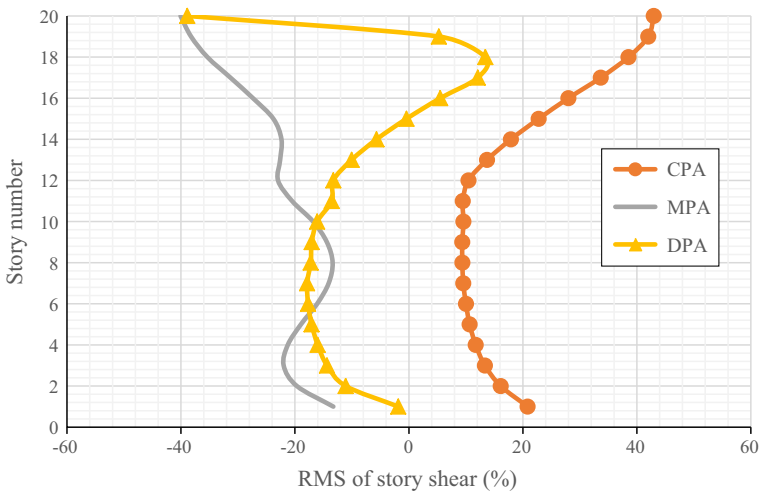


**Fig. 14** The story-wise RMS values for a 15% eccentricity, 20-story building, story shear

6.5.2 Story PHR estimation

As shown in Figs. 16, 17, 18, 19, the relative error of the estimated story PHRs are in most cases positive. It shows that the estimated value is too small in those cases (see Eq. 20). Therefore, it seems appropriate to multiply the estimated values by a value larger than unity, say by  $\sum_{j=1}^n \alpha_j$ , to reduce the estimation error. Then,  $\overline{PHR}_i$ , that is the modified  $\overline{PHR}_i$ , is calculated using Eq. (23):

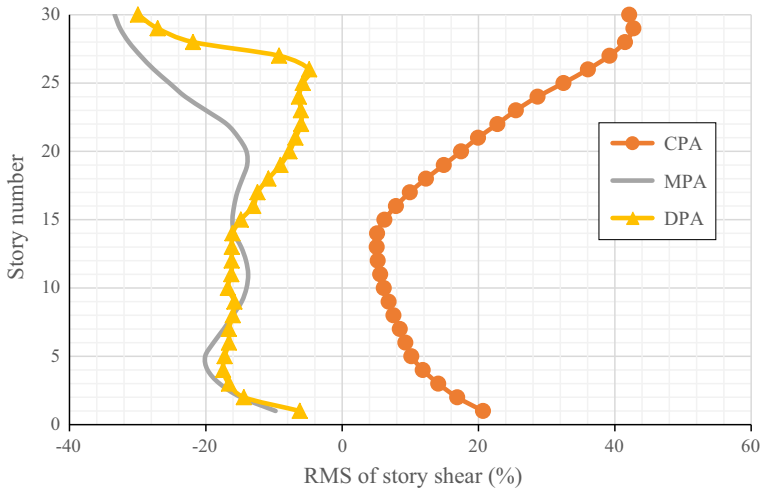


**Fig. 15** The story-wise RMS values for a 15% eccentricity, 30-story building, story shear

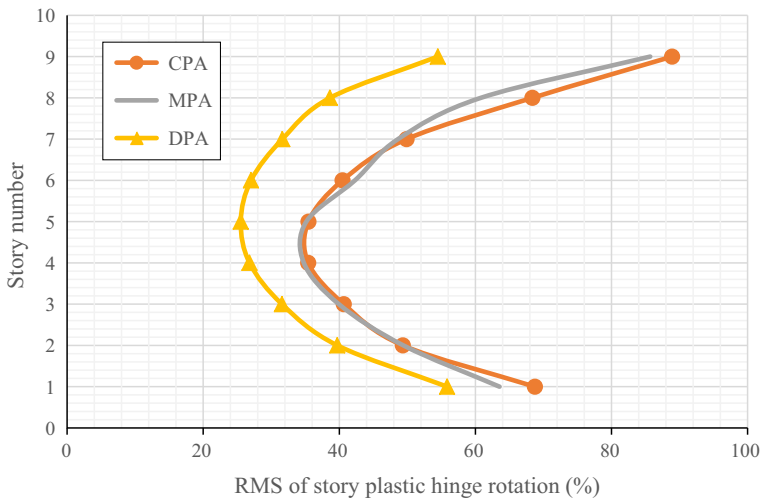


**Fig. 16** The story-wise RMS values for a 15% eccentricity, 10-story building, story plastic hinge rotation

$$\overline{PHR}_i = PHR_i \sum_{j=1}^n \alpha_j \tag{23}$$

The resultant values of RMS errors for  $\overline{PHR}_i$ , as well as the maximum story RMS error, of DPA5 are exhibited in Table 18 for the studied buildings in comparison to CPA and MPA. The resultant RMS error of DPA5 is reduced to less than 40% after modification.



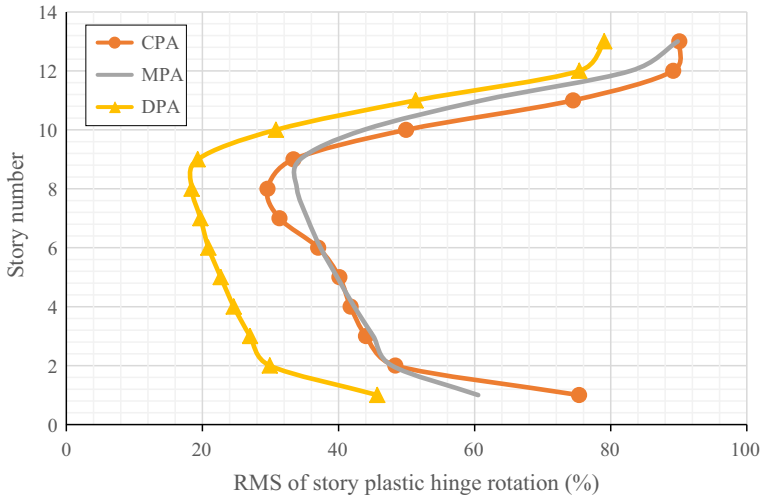


**Fig. 17** The story-wise RMS values for a 15% eccentricity, 15-story building, story plastic hinge rotation

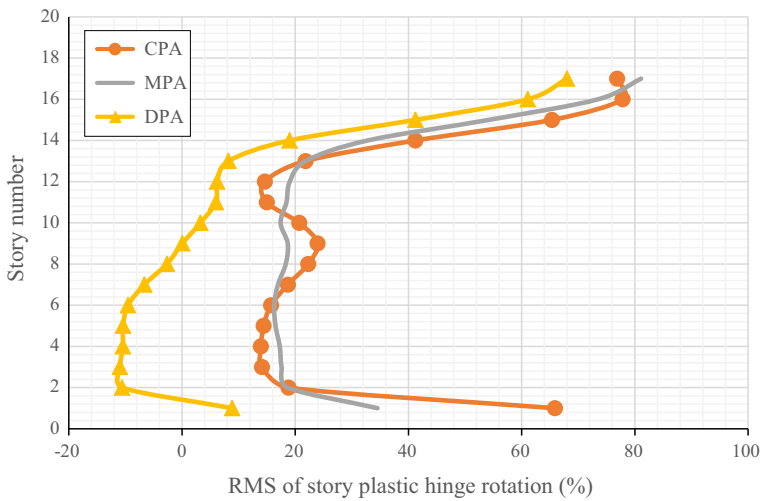


**Fig. 18** The story-wise RMS values for a 15% eccentricity, 20-story building, story plastic hinge rotation

### 7 Conclusions

The drift pushover method, developed previously by the authors for 2D structures, was extended in this paper to 3D buildings focusing on torsional structures. In this method, the story drifts are calculated in each mode using conventional relations of the modal analysis. They are then combined using the proposed procedure that retains their signs. The push-over analysis then is implemented using the equivalent lateral forces that produce the same drifts. Six approaches for combination of the modal story drifts and two approaches for determination of the equivalent lateral forces were examined.

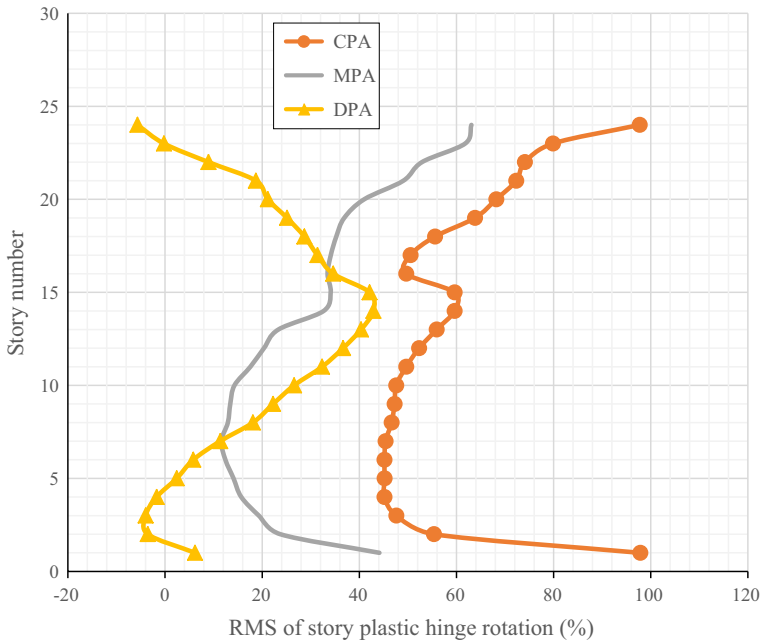


**Fig. 19** The story-wise RMS values for a 15% eccentricity, 30-story building, story plastic hinge rotation

**Table 16** Values of  $\alpha_j$  for DPA5

Mode no.	10-story			15-story			20-story			30-story		
	1	2	3	1	2	3	1	2	3	1	2	3
$\alpha_j$	1.04	0.05	0.01	1.04	0.05	0.01	1.04	0.05	0.01	0.99	0.14	0.05

**Table 17** Comparison of resultant and maximum RMS errors (%) in the upper half stories for the story shears, 15% eccentricity

Method	Itant RMS				Max RMS			
	CPA	MPA	DPA	DPA (modified)	CPA	MPA	DPA	DPA (modified)
20-story	28.69	29.27	18.07	12.10	42.96	40.07	38.89	34.22
30-story	35.26	28.24	20.96	13.74	42.73	33.37	29.96	20.73

The DPA approach with the superior accuracy with regard to other well-known push-over methods was identified in comparison to the exact nonlinear dynamic response. The accuracy analysis was performed by calculating story displacements, shears, and plastic hinge rotations of 10–30 stories buildings with increasing mass eccentricities under several consistent earthquakes.

**Table 18** Comparison of the resultant and maximum RMS errors (%) of the story PHR's, 15% eccentricity

Method	Resultant RMS				Max RMS			
	CPA	MPA	DPA	DPA (modified)	CPA	MPA	DPA	DPA (modified)
10-story	55.8	55	38.4	32.8	88.9	85.6	55.8	51.44
15-story	56.7	53.3	41	36.7	90.08	89.8	79	76.95
20-story	39.3	35.3	26	26	81.09	77.8	68.02	64.82
30-story	60.79	33.69	24.11	18.81	97.84	63.08	42.91	32.63

In the proposed method, the modal combination of story drifts with retaining their signs, was shown to be best implemented if the modal drifts were weighted based on the modal accelerations and were calibrated using the mode shape amplitudes at the roof of the buildings. It was shown that the proposed DPA procedure had a better accuracy regardless of the value of the torsional eccentricity. It performed better than CPA and MPA methods both regarding the resultant RMS error of responses and height-wise distribution of RMS in each building. Therefore, the proposed DPA method can act as an effective and efficient tool in estimation of maximum seismic responses of unsymmetric plan buildings with a better accuracy compared to the major existing methods.

While the resultant RMS errors of story displacements and shears are small enough for all of the building and eccentricity cases, they are larger for story plastic hinge rotations in the proposed method. Moreover, the story RMS error is too large in some cases. Further development of the study should focus on improving the accuracy of story RMS or distribution of RMS along height of the torsional buildings.

## References

- Albanesi T, Biondi S, Petrangeli M (2002) Pushover analysis: an energy based approach. In: Proceedings of the twelfth European conference on earthquake engineering, London, United Kingdom, Paper No. 605
- American Institute of Steel Construction (2010) Specification for structural steel buildings. ANSI/AISC 360-10, Chicago, IL
- American Society of Civil Engineers (2010) Minimum design loads for buildings and other structures: Second Printing. ASCE7-10
- American Society of Civil Engineers (2014) Seismic evaluation and retrofit of existing buildings. ASCE SEI 41-13
- Antoniou S, Pinho R (2004) Development and verification of a displacement-based adaptive pushover procedure. *J Earthq Eng* 8:643–661
- Behnamfar F, Taherian SM, Sahraei A (2016) Enhanced nonlinear static analysis with the drift pushover procedure for tall buildings. *Bull Earthq Eng* 14:3025–3046
- Bracci JM, Kunnath SK, Reinhorn AM (1997) Seismic performance and retrofit evaluation of reinforced concrete structures. *J Struct Eng ASCE* 123:3–10
- Chopra AK, Goel RK (2000) Evaluation of NSP to estimate seismic deformation: SDF systems. *J Struct Eng ASCE* 126:482–490
- Chopra AK, Goel RK (2004) A modal pushover analysis procedure for estimating seismic demands for unsymmetric-plan buildings. *Earthq Eng Vib* 33:903–927
- Fajfar P, Marusic D, Perus I (2005a) Torsional effects in the pushover-based seismic analysis of buildings. *J Earthq Eng* 9(6):831–854
- Fajfar P, Marusic D, Perus I (2005b) The extension of  $N_2$  method to asymmetric buildings. In: Proceedings of the 4th European workshop on the seismic behaviour of irregular and complex structures, Thessaloniki

- Gupta B (1999) Enhanced pushover procedure and inelastic demand estimation for performance-based seismic evaluation of buildings, Ph.D. Dissertation, University of Central Florida, Orlando, FL
- Gupta B, Kunnath S (1999) Pushover analysis of isolated flexural reinforced concrete walls. 1999 New Orleans Structures Congress
- Mazzoni S, McKenna F, Scott M, Fenves G, Jeremic B (2006) OpenSees command language manual. Pacific Earthquake Engineering Research Center (PEER), University of California, Berkeley, California
- Moghadam AS, Tso WK (2000a) Pushover analysis for asymmetric and set-back multi-story buildings. In: Proceedings of the 12th world conference on earthquake engineering, Auckland, New Zealand
- Moghadam AS, Tso WK (2000b) 3-D push-over analysis for damage assessment of buildings. *J Seismol Earthq Eng* 2(3):23–31
- Pacific Earthquake Engineering Research Center (2016) PEER ground motion database. <http://ngawest2.berkeley.edu/>
- Parducci A, Comodini F, Lucarelli M, Mezzi M, Tomassoli E (2006) Energy-based nonlinear static analysis. In: First European conference on earthquake engineering and seismology
- Poursha M, Khoshnoudian F, Moghadam A (2009) A consecutive modal pushover procedure for estimating the seismic demands of tall buildings. *Eng Struct* 31:591–599
- Requena M, D’Ayala G (2000) Evaluation of a simplified method for the determination of the nonlinear seismic response of RC frames. In: Proceedings of the twelfth world conference on earthquake engineering, Auckland, New Zealand, Paper No. 2109
- Reyes JC, Chopra AK (2011a) Three-dimensional modal pushover analysis for buildings subjected to two components of ground motion, including its evaluation for tall buildings. *Earthq Eng Eng Vib* 40:789–806
- Reyes JC, Chopra AK (2011b) Evaluation of three-dimensional modal pushover analysis for unsymmetric-plan buildings subjected to two components of ground motion. *Earthq Eng Eng Vib* 40:1475–1494
- Sahraei A, Behnamfar F (2014) A drift pushover analysis procedure for estimating the seismic demands of buildings. *Earthq Spectra* 30:1601–1618
- Tjhin T, Aschheim M, Hernández-Montes E (2005) Estimates of peak roof displacement using “equivalent” single degree of freedom systems. *J Struct Eng ASCE* 131:517–522
- Tso WK, Moghadam AS (1997) Seismic response of asymmetrical buildings using push-over analysis. In: Proceedings of workshop on seismic design methodologies for the next generation of codes, Bled, Slovenia